Cancer Cell
Article

Proinvasion Metastasis Drivers in Early-Stage Melanoma Are Oncogenes

Kenneth L. Scott,[1,2,10,11] Cristina Nogueira,[1,2,3,10] Timothy P. Heffernan,[1,2,10] Remco van Doorn,[2,4] Sabin Dhakal,[1,2] Jason A. Hanna,[5] Chengyin Min,[1,2] Mariela Jaskelioff,[1,2] Yonghong Xiao,[1] Chang-Jiun Wu,[1,2] Lisa A. Cameron,[6] Samuel R. Perry,[1] Rhamy Zeid,[1] Tamar Feinberg,[1,2] Minjung Kim,[1,2,12] George Vande Woude,[7] Scott R. Granter,[8] Marcus Bosenberg,[5] Gerald C. Chu,[1,2,8] Ronald A. DePinho,[1,2] David L. Rimm,[5] and Lynda Chin[1,2,9,*]

[1]Belfer Institute for Applied Cancer Science
[2]Department of Medical Oncology
Dana-Farber Cancer Institute, Boston, MA 02115, USA
[3]Institute of Molecular Pathology and Immunology of the University of Porto, (IPATIMUP)/Medical Faculty, University of Porto, 4200-465 Porto, Portugal
[4]Department of Dermatology, Leiden University Medical Center, 2300 RC Leiden, The Netherlands
[5]Department of Pathology, Yale University Medical School, New Haven, CT 06510-3206, USA
[6]Confocal and Light Microscopy Core, Dana-Farber Cancer Institute, Boston, MA 02115, USA
[7]Van Andel Research Institute, Grand Rapids, MI 49503, USA
[8]Department of Pathology, Brigham and Women's Hospital
[9]Department of Dermatology, Harvard Medical School
Boston, MA 02115, USA
[10]These authors contributed equally to this work
[11]Present address: Department of Molecular and Human Genetics, Baylor College of Medicine, One Baylor Plaza, Houston, TX 77030, USA
[12]Present address: Department of Molecular Oncology, H. Lee Moffitt Cancer Center and Research Institute, Tampa, FL 33612, USA
*Correspondence: lynda_chin@dfci.harvard.edu
DOI 10.1016/j.ccr.2011.05.025

SUMMARY

Clinical and genomic evidence suggests that the metastatic potential of a primary tumor may be dictated by prometastatic events that have additional oncogenic capability. To test this "deterministic" hypothesis, we adopted a comparative oncogenomics-guided function-based strategy involving: (1) comparison of global transcriptomes of two genetically engineered mouse models with contrasting metastatic potential, (2) genomic and transcriptomic profiles of human melanoma, (3) functional genetic screen for enhancers of cell invasion, and (4) evidence of expression selection in human melanoma tissues. This integrated effort identified six genes that are potently proinvasive and oncogenic. Furthermore, we show that one such gene, *ACP5*, confers spontaneous metastasis in vivo, engages a key pathway governing metastasis, and is prognostic in human primary melanomas.

INTRODUCTION

Cancers are highly heterogeneous on both the genomic and cellular levels such that similarly staged early disease can exhibit radically different clinical outcomes—from cure following surgical removal of the primary tumor to death within months of diagnosis due to widespread metastasis. Metastasis is responsible for the majority of cancer-related mortality and involves multiple interrelated steps by which primary tumor cells spread to establish cancerous lesions at distant sites (Gupta and Massague, 2006). To become metastatic, tumor cells acquire a number of biological capabilities to overcome barriers of dissemination and distant growth such as invasion, anoikis resistance, extravasation, colonization, and growth in new

Significance

Early-stage melanoma is often cured by surgical excision, yet some cases without clinical evidence of dissemination recur with lethal metastatic disease despite successful surgical removal of the primary tumor. Elucidation of the molecular basis underlying such aggressive biology has been a long-standing focus, with the goal of identifying prognostic biomarkers and rational therapeutics for high-risk patients diagnosed with early-stage disease who are in need of further treatment in adjuvant setting. This study illustrates how one can exploit and integrate genetically engineered mouse models, cross-species cancer genomics knowledge, and functional screens to identify robust proinvasion drivers of metastasis that are also bona fide oncogenes.

microenvironments. Each of these biological attributes can be conferred by genetic or epigenetic events observed in tumors (Hanahan and Weinberg, 2011), supporting the thesis that biological heterogeneity of cancers, including metastatic potential, is dictated by underlying genomic alterations.

Although significant data exist in support of a classical model of stepwise accumulation of genetic events that endow increasing malignant potential, the identification of extensive genome rearrangements in early-stage cancers (driven in part by telomere crisis) (Rudolph et al., 2001; Chin et al., 2004) raises the possibility that some tumors may acquire genomic alterations with significant metastatic potential early in their evolution. Such tumors would inherently carry higher risk for metastasis despite early diagnoses. This deterministic model is consistent with the finding that transcriptomic profiles of primary tumors share striking resemblance with their metastatic lesions (Perou et al., 2000), and gene expression patterns of the primary bulk tumor can predict the likelihood of recurrence or metastatic spread, e.g., MammaPrint and OncotypeDx (van't Veer et al., 2002; Paik et al., 2004). Furthermore, the prognostic significance of these gene expression signatures supports the view that information on metastatic propensity is encoded in the bulk of the primary tumor (van 't Veer et al., 2002; van de Vijver et al., 2002; Ramaswamy et al., 2003).

Together, these observations lead one to posit that prometastatic genetic alterations acquired early at primary tumor stage might themselves be classical oncogenes and tumor suppressor genes that can confer a selective growth advantage during tumorigenesis, and if so, such genes would be subject to recurrent genomic alterations in cancer (i.e., amplification and loss). Therefore, the existence and identification of such prometastasis oncogenes could provide both prognostic markers as well as therapeutic targets for inherently aggressive early-stage cancers. In this study, using melanoma as a disease model given its cardinal feature of high metastatic propensity, we sought to validate the concept of "oncogenic driver of metastasis" or "metastasis oncogenes" through systematic identification of putative metastasis driving genes that also confer transforming oncogenic activity in early-stage cancers.

RESULTS

Evolutionarily Conserved, Differentially Expressed Genes with Metastatic Potential

The enormous genomic complexity of human melanoma and the less than complete certainty surrounding occult metastatic disease in any given human patient prompted us to compare two extensively characterized genetically engineered mouse (GEM) models of human melanoma with distinct metastatic profiles. The selected melanoma models are: (1) the *HRAS*^{V12G}-driven mouse melanoma model (*Tyr-rtTA;Tet-HRAS*^{V12G}*;INK4A/ARF*$^{-/-}$, hereafter "iHRAS*"), which develops aggressive cutaneous melanomas that do not metastasize (Chin et al., 1997, 1999); and (2) a *MET*-driven GEM model (*Tyr-rtTA;Tet-Met;INK4A/ARF*$^{-/-}$, hereafter "iMet"), which develops metastatic melanomas. The iMet model expresses an inducible c-*MET* transgene (Tet-Met) and is constructed following a similar engineering strategy used for the iHRAS* model (Ganss et al., 1994; Chin et al., 1997, 1999) (see Supplemental Experimental Procedures available online). Tet-Met transgenic animals were bred with transgenic mice carrying the reverse tetracycline transactivator under the control of tyrosinase gene promoter-enhancer elements (designated *Tyr-rtTA*) (Gossen et al., 1995). Given the frequency and demonstrated relevance of *INK4A/ARF* deletions in melanoma (Hussussian et al., 1994; Kamb et al., 1994), these compound transgenic alleles were further intercrossed onto an *INK4A/ARF* null background to generate cohorts of single- and double-transgenic mice (designated iMet) deficient for *INK4A/ARF* whose melanocytes express *MET* upon induction with doxycycline (Figure 1A).

iMet mice develop melanomas at sites of skin wounding with an average latency of 12 weeks (Table S1). These lesions are positive for prototypical melanocyte markers and express phospho-Met (c-Met) receptor and its ligand hepatocyte growth factor (HGF) (Figures 1B and 1C; Figures S1A and S1B). These iMet melanomas uniformly metastasize to lymph nodes and show occasional dissemination to the adrenal glands and lung parenchyma, which are common sites for metastases in human melanoma (Figure 1D). In sharp contrast the iHRAS* melanoma model develops aggressive cutaneous melanomas that do not metastasize (Chin et al., 1997, 1999). Consistent with the contrasting metastatic potential of iMet and iHRAS* primary tumors, only iMet melanoma-derived cell lines were able to seed and grow to large macroscopic lesions in tail vein experimental metastasis assays (Figure S1C).

Using these two GEM models as "extreme cases," we compared the transcriptomic profiles of primary cutaneous melanomas from iHRAS* and iMet models to define 1597 gene probe sets with $\geq$2-fold differential expression at a false discovery rate <0.05. This list of differentially expressed genes was next intersected with genes residing in recurrent copy number aberrations (CNAs) in human metastatic melanoma (GEO accession #GSE7606) and/or genes exhibiting significant differential expression between primary and metastatic melanomas in human (Kabbarah et al., 2010). This comparative oncogenomics analysis led to a list of 360 genes comprised of 295 upregulated/amplified and 65 downregulated/deleted candidates (Figure 2A; Table S2), representing differentially expressed genes in primary melanoma that are correlated with metastatic potential. Compared with the 1597 probe set, this cross-species intersected list of 360 genes was significantly more enriched for cancer-relevant functional networks based on Ingenuity Pathway Analysis (IPA) (Figure S2A).

Identification of Proinvasion Oncogenes

From the aforementioned cross-species triangulated gene list for metastatic potential, we set out to identify functionally active metastasis drivers in primary melanomas following the experimental outline in Figure 2B. In particular we designed a genetic screen for invasion based on the rationale that the ability of primary melanoma cells to invade downward into the dermis and subcutis is significantly correlated with metastasis, and a primary melanoma with proinvasive genetic events is more likely to metastasize early; hence, we postulated that metastasis drivers in such primary melanoma would harbor proinvasive activity. Here, we elected to focus on the 295 upregulated genes using a gain-of-function screening design given their possible therapeutic potential. The human ORFeome collection

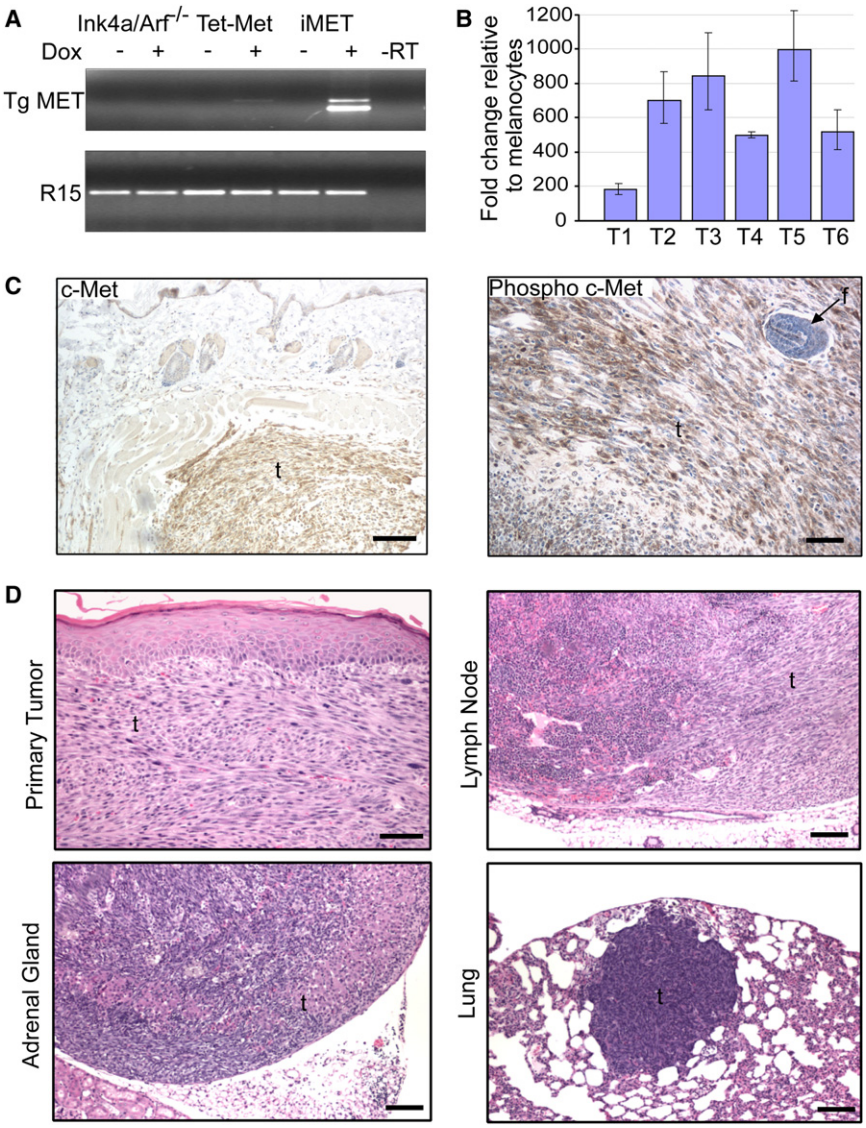

Figure 1. Melanocyte-Specific *MET* Expression Promotes Formation of Cutaneous Metastatic Melanoma

(A) Melanocytes were harvested from the indicated animals (*INK4A/ARF*$^{-/-}$, Tet-Met, and iMet) and adapted to culture for total RNA extraction following treatment with or without doxycycline (Dox). Expression of MET (Tg MET) was assayed by RT-PCR using transgene-specific primers. R15, ribosomal protein R15 internal control; -RT, no reverse transcriptase PCR control.

(B) qRT-PCR was performed to analyze *HGF* expression in *MET*-induced primary melanomas (T1–T6). Tumor expression data are normalized to expression in two *INK4A/ARF*$^{-/-}$ melanocyte cell lines. Error bars indicate ± SD.

(C) Immunohistochemical staining of total Met (c-Met) and phosphorylated (Phospho) c-Met in a MET-induced primary melanoma. The arrow points to a follicle (f). Scale bars, 100 μm (left) and 50 μm (right).

(D) H&E sections of a primary cutaneous spindle cell melanoma in the dorsal skin of an iMet transgenic mouse induced with doxycycline and distal metastases residing in lymph node, adrenal gland, and lung. Scale bars, 50 μm (primary tumor [t]) and 100 μm (metastases).

See also Figure S1 and Table S1.

c-met (http://horfdb.dfci.harvard.edu/) contained 230 open reading frame (ORF) cDNAs corresponding to 199 of the 295 unique upregulated/amplified candidates (Table S3), which were then transferred to a lentiviral expression system for transduction into HMEL468 (PMEL/hTERT/CDK4(R24C)/p53DD), a TERT-immortalized primary human melanocyte line engineered to express *BRAF*^{V600E} (Garraway et al., 2005). For the primary screen we utilized a 96-well transwell invasion assay with fluorometric readout to measure the ability of candidate genes to enhance migration and invasion of HMEL468 through Matrigel, which simulates extracellular matrix. Lentiviral expression vectors encoding GFP and *NEDD9* (Kim et al., 2006; O'Neill et al., 2007; Sanz-Moreno et al., 2008; Izumchenko et al., 2009) were used as negative and positive controls, respectively. The primary screen was performed in duplicate, and 45 candidates that reproducibly scored two standard deviations from the GFP control were considered as primary screen hits (Figure S2B and Table S3). Secondary validation of these 45 candidate genes was performed by assaying their invasive ability in standard 24-well Matrigel invasion chambers, together with parallel sequencing and expression verification (see Supplemental Experimental Procedures), yielding 18 genes (Table S4) possessing >2-fold enhancement of invasion compared to the GFP control (Figure 2C and Table 1). As a frame of reference, the positive control prometastasis gene *NEDD9*, which has been shown to be required for cell movement (Sanz-Moreno et al., 2008) and in vivo metastasis of breast cancers (Izumchenko et al., 2009), enhanced invasion by 1.5-fold in this system (data not shown).

To prioritize downstream validation efforts, we next assayed the 18 candidates for ability to confer a 2-fold increase of invasion in a second melanoma cell system, WM115. This identified 11 robust proinvasion genes (Table 1). Mindful of the artificial nature of in vitro invasion screen and limitation of an overexpression system, we then interrogated the expression patterns of these proinvasion genes in human melanocytic lesions for evidence of human relevance, specifically increasing expression from benign to malignant and/or from primary to metastasis lesions as criteria for clinicopathological validation. To this end, we rigorously screened commercially available antibodies and successfully qualified and optimized conditions of 7 antibodies for proteins encoded by 7 of the 11 genes for quantitative immunofluorescence staining on formalin-fixed paraffin-embedded tissue. Using the Automated Quantitative Analysis (AQUA®) platform (Camp et al., 2002), we quantitated protein expression

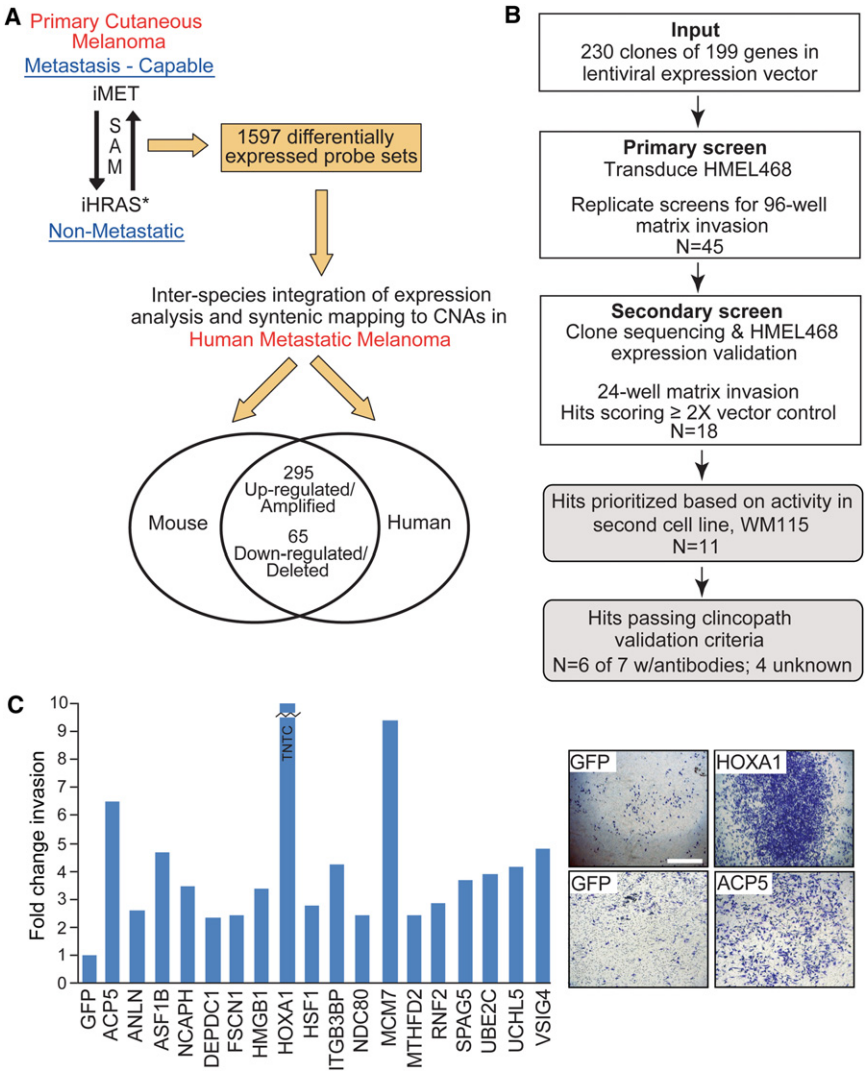

Figure 2. Multidimensional Genomic Analyses and Low-Complexity Functional Genetic Screen for Cell Invasion

(A) Schematic illustrating the integrative cross-species oncogenomics comparison.

(B) Flowchart depicting the low-complexity genetic screen for invasion and validation processes.

(C) Histogram of 18 proinvasion genes satisfying sequencing, expression, and secondary screen verification efforts. Representative invasion chamber images for HMEL468 cells stably expressing *HOXA1* and *ACP5* are shown. GFP, negative control; TNTC, too numerous to count. Scale bar, 1.6 mm.

See also Figure S2 and Tables S2–S4.

levels on the Yale Melanoma Progression Tissue Microarray (YTMA98) containing 20 specimens each of benign nevi, primary melanoma, and melanoma metastases. As summarized in Table 1, proteins encoded by six of seven (*ACP5*, *FSCN1*, *HOXA1*, *HSF1*, *NDC80*, *VSIG4*) proinvasion genes showed significantly higher expression across the benign-to-malignant and/or primary-to-metastasis transitions in human (Table 1; Figure S3), qualifying them as validated proinvasion genes in human melanomas.

The acquisition of metastasis drivers in some early-stage tumors might reflect their roles as bona fide oncogenes that could provide a proliferative advantage to the emergent primary tumors as speculated by Bernards and Weinberg (2002). To test this hypothesis, we examined the oncogenic potential of the six validated proinvasion genes by assaying their requirement in maintaining the tumorigenic phenotype of established human melanoma cells in vitro and their ability to transform immortalized human melanocytes in vivo. For example, using anchorage-independent growth as a surrogate for tumorigenic phenotype, depletion of *ACP5* using two independent shRNAs in the human melanoma cell line 1205Lu resulted in a 56% reduction in soft-agar colony formation ($p = 0.0001$) (Figure 3A). Conversely, HMEL468 melanocytes (1×10^6 cells/injection) stably expressing *ACP5* became robustly tumorigenic when subcutaneously implanted into the right flank of athymic nude mice ($p = 0.0012$) (Figure 3B). Importantly, extending these assays to the remaining five proinvasion genes, we found that knockdown of all six in M619 and C918 human melanoma cells significantly decreased colony formation when compared with nontargeting (shGFP) shRNA (Figure 3C; Figure S4). Similarly, mice injected with HMEL468 cells overexpressing each of the six genes developed tumors, compared to none of the animals injected with GFP control HMEL468 cells after 30 weeks of observation (Figure 3D). Together, these complementary loss- and gain-of-function studies demonstrated unequivocally that all six of these proinvasion genes are oncogenic. These results are striking given that transforming activity of these genes was not screened for in the course of their identification.

In summary, from the initial cross-species differentially expressed list of 199 genes enlisted into the functional screen for cell invasion, 18 candidate metastasis oncogenes were identified. Of these, seven candidates were prioritized for multilevel functional and clinicopathological validation; six were confirmed as potent proinvasion oncogenes, capable of robust transforming and invasive activities in immortalized nontransformed human melanocytes and whose expressions positively correlated with human melanoma transformation or progression.

Functional and Clinical Validation of *ACP5*

Our integrated functional genomics screen and validation above have identified six proinvasion oncogenes that are posited to confer enhanced metastasis risk in vivo and, therefore, carry prognostic significance in patients diagnosed with primary melanomas. To seek evidence in support of this, we next focused on *ACP5* as a proof-of-concept example based on the observations

Table 1. Invasion Validation and Progression-Correlated Expression Analysis

Metastasis Oncogene Candidates	Gene ID	Gene Name	HMEL468 Invasion Screen	Invasion Activity in WM115	Clinicopathological Validation[a]			Oncogenic In Vivo
					Transformation[b]	Progression[c]	Passed?	
ACP5	54	Acid phosphatase 5, tartrate resistant	6.5X	2.1X	p = 0.001	p = 0.026	Yes	Yes
FSCN1	6624	Fascin homolog 1, actin-bundling protein	2.4X	2.2X	ns	p = 0.026	Yes	Yes
HOXA1	3198	Homeobox A1	TNTC	6.1X	p < 0.001	ns	Yes	Yes
HSF1	3297	Heat shock transcription factor 1	2.8X	4.4X	p = 0.003	ns	Yes	Yes
NDC80	10403	*ndc80* homolog, kinetochore component	2.4X	2.2X	ns	p = 0.034	Yes	Yes
VSIG4	11326	V set and immunoglobulin domain cont. 4	4.8X	2.1X	p < 0.001	ns	Yes	Yes
NCAPH	23397	Non-SMC condensin I complex, subunit H	3.5X	2.1X	ns	ns	No	nt
ASF1B	55723	ASF1 anti-silencing function 1 homolog B	4.7X	2.0X	No antibody			nf
MTHFD2	10797	Methylenetetrahydrofolate dehydrogenase	2.4X	2.5X	No antibody			nf
RNF2	6045	Ring finger protein 2	2.9X	3.4X	No antibody			nf
SPAG5	10615	Sperm associated antigen 5	3.2X	2.5X	No antibody			nf
ANLN	54443	Anillin, actin binding protein	2.6X	ns				
DEPDC1	55635	DEP domain containing 1	2.3X	ns				
HMGB1	3146	High-mobility group box 1	3.4X	ns				
ITGB3BP	23421	Integrin beta 3 binding protein	4.2X	ns				
MCM7	4176	Minichromosome maintenance complex 7	9.4X	ns				
UBE2C	11065	Ubiquitin-conjugating enzyme E2C	3.9X	ns				
UCHL5	51377	Ubiquitin carboxyl-terminal hydrolase L5	4.1X	ns				

nt, not tested; ns, not significant; nf, not followed up; TNTC, too numerous to count.
[a] Fisher's test for significance between means.
[b] Associated with transformation means primary or Mets greater than nevi.
[c] Associated with progression means Mets greater than primary.

that: (1) *ACP5* was the only gene exhibiting significant expression correlation with transformation as well as progression (Table 1); and (2) Acp5 protein expression has been used as a histochemical marker of osteoclastic activity, which is increased in conditions of bone diseases including bone metastases (Halleen et al., 2001; Capeller et al., 2003; Lyubimova et al., 2004).

To investigate *ACP5*'s ability to drive distal metastasis in vivo, we overexpressed *ACP5* or GFP control in the human melanoma cell line 1205Lu, which shows minimal to no distal metastasis from skin tumor sites. One million cells were then implanted into a subcutaneous site in the skin on one flank of athymic nude mice (n = 5) and followed for primary tumor growth. When tumor size reached 2 cm in one dimension, the maximum size allowed by our experimental protocol, animals were sacrificed and examined for macrometastasis and micrometastasis in lymph nodes and distal organ systems. Consistent with its invasive activity, animals bearing *ACP5*-expressing melanomas in the subcutaneous sites developed spontaneous metastasis to the lung and lymph nodes (n = 2) (Figure 4A), whereas none in the control cohort harbored any metastatic lesion despite similar tumor penetrance in both cohorts (n = 5 each). Additionally, based on the prognostic significance of these genes in human breast cancers (see below), we also utilized NB008 (mTerc$^{-/-}$, p53$^{+/-}$; mTerc), a well-characterized, nonmetastatic cell line originating from a spontaneous murine mammary adenocarcinoma (mTerc$^{-/-}$, p53$^{+/-}$) engineered to reexpress mTerc. Specifically, GFP-labeled NB008 cells stably expressing *ACP5* or vector control were orthotopically implanted into the right inguinal mammary fat pad of athymic nude mice. Macroscopic GFP-positive lesions in the lungs were scored at necropsy when primary mammary tumors reached 2 cm (Figure 4B). As shown by Kaplan-Meier metastasis-free survival analysis,

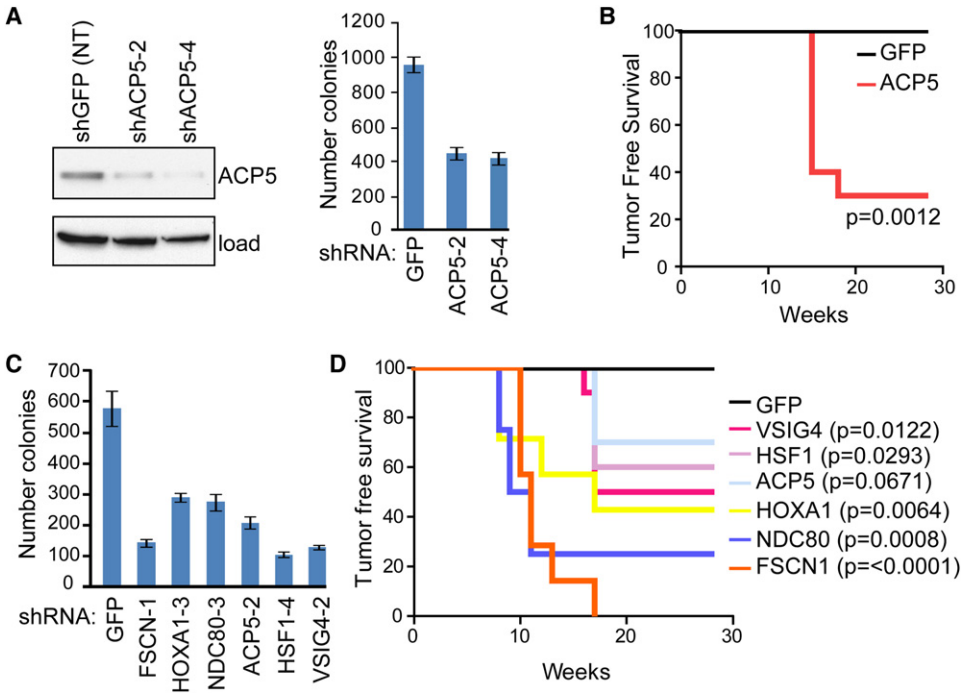

Figure 3. Assessment of Oncogenic Activity by Proinvasion Genes

(A) 1205Lu melanoma cells expressing nontargeting control (shGFP; NT) or individual shRNA hairpins against *ACP5* (shACP5-2 and -4) were assayed for effects on anchorage-independent growth in soft agar. Immunoblot depicts Acp5 protein knockdown with indicated hairpins.

(B) Kaplan-Meier tumor-free survival analysis for xenograft assays in Ncr-Nude mice using nontumorigenic HMEL468 cells (1×10^6 cells/injection site) stably expressing GFP or *ACP5* (n = 10 each). p value calculated by log rank test.

(C) M619 melanoma cells expressing nontargeting control (GFP) or individual shRNA hairpins against the indicated candidates were assayed for effects on anchorage-independent growth in soft agar as in (A). See Figure S4 for additional data using C918 melanoma cells and complementary knockdown verification data.

(D) Kaplan-Meier tumor-free survival analysis for xenograft assays in Ncr-Nude mice using nontumorigenic HMEL468 cells stably expressing the indicated genes as in (B). Log rank-calculated p values for individual candidates indicated at right of plot. Error bars indicate ± SD.

GFP-positive macrometastasis was detected in the lungs of 89% (eight of nine) of mice bearing *ACP5*-expressing tumors, whereas none (zero of eight) of the animals injected with control tumor cells presented with lung nodules (p = 0.0003; Figure 4B). Histopathological examination confirmed presence of macrometastases and micrometastases (Figure 4C). Together, these results show that *ACP5* is a bona fide metastasis driver in vivo.

Next, to investigate the prognostic significance of *ACP5* expression in human primary melanomas, we again employed the quantitative immunofluorescence measurement of Acp5 protein expression on a tissue microarray (YTMA59) containing 196 cases of primary melanomas and 299 cases of metastatic melanomas annotated for survival outcome (Berger et al., 2005; Gould Rothberg et al., 2009). As observed in the clinicopathological validation study (Figure S3), Acp5 staining was primarily cytoplasmic, and the differential distributions of staining intensity were significantly higher in the metastatic lesions compared to primary specimens (Figure 5A) (ANOVA, $p < 0.0001$). Importantly, the Acp5 protein level in primary melanomas correlates with survival of patients, for which a significantly shorter melanoma-specific survival was observed in cases with higher cytoplasmic Acp5 levels (log rank, p = 0.0258) (Figures 5B and 5C; Figure S5). Therefore, collectively, our data show that *ACP5* is not only a proinvasion oncogene but also a prognostic biomarker in human primary melanomas.

On the cell biological level, overexpression and RNAi knockdown of *ACP5* resulted in striking morphological changes such as cell spreading and cell rounding, respectively (Figure 6A), prompting us to consider the possibility that *ACP5* could modulate phosphorylation of focal adhesion complexes that are integral to cell attachment and motility. Indeed, overexpression of *ACP5* in melanoma cells led to a reproducible decrease in focal adhesion kinase (FAK) autophosphorylation at Tyr397 (Figure 6B) and global FAK tyrosine phosphorylation beyond its autophosphorylation site (Figure 6C). Similar analysis uncovered a more significant effect of *ACP5* overexpression on tyrosine phosphorylation of Paxillin (PAX) (Figure 6C), including Tyr118 (Figure S6), which is thought to serve as a critical docking site for other signaling molecules. Live-cell imaging of *ACP5* overexpressing cells translated these biochemical changes to increased cell movement (Movies S1 and S2), consistent with our data on *ACP5*'s activity on cell invasion. Given the literature implicating the FAK complex activity in metastasis (Zheng and Lu, 2009), this mechanistic link thus further substantiates the functional role of *ACP5* in invasion and points to the FAK complex as a possible point of therapeutic intervention in high-risk primary melanoma with high *ACP5* expression.

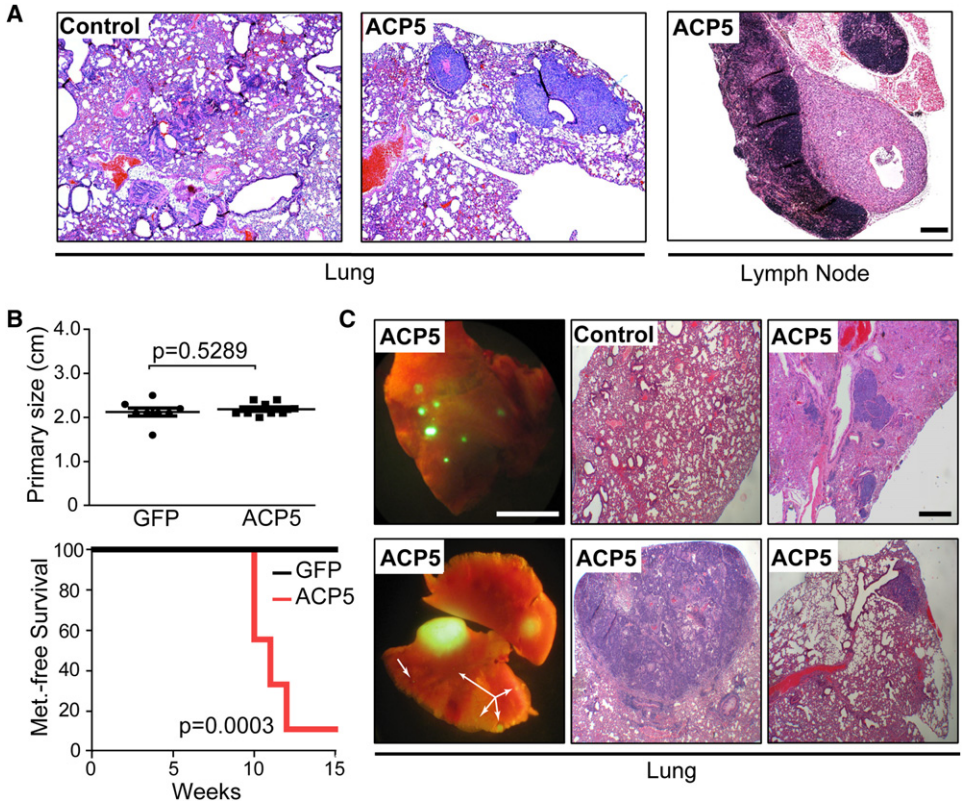

Figure 4. In Vivo Metastasis Studies

(A) Representative H&E of lung and lymph node metastases in athymic mice (two of five) harboring subcutaneous tumors generated from 1205Lu melanoma cells expressing *ACP5*. No metastases (zero of five animals) were detected in the GFP-expressing control cohort. Scale bar, 200 μm.

(B) Mammary fat pad metastasis assay using GFP-positive nonmetastatic murine breast adenocarcinoma cells (NB008; 2×10^4 cells/injection site) stably expressing vector control or *ACP5*. Endpoint primary tumor size (top) and Kaplan-Meier metastasis-free survival analysis (bottom) are shown. p values calculated by two-tailed Student's t test (top) and log rank (bottom).

(C) Representative images of GFP-positive lung metastases and H&E sections of infiltrated lung from the *ACP5* cohort. Arrows denote micrometastases. Scale bars, 5.5 mm (left two panels) 300 μm (right four H&E panels).

Metastasis Oncogenes Are Not Lineage Specific

Although the majority of proinvasion genes identified from our integrated functional genetic screen have not been linked to metastasis (see Discussion), the actin-bundling protein Fscn1 is reported to be prognostic in numerous cancer types (Hashimoto et al., 2005), and recently shown to be required for metastasis (Chen et al., 2010). This led us to explore the prognostic relevance of these proinvasion genes in other tumor types using RNA expression, given the limitation of antibody reagent for quantitative protein-based assays. We focused specifically on breast cancer based on the availability of three independent cohorts of transcriptome data sets on stage I/II breast adenocarcinomas with outcome (recurrence or metastasis-free survival) annotation (van de Vijver et al., 2002; Pawitan et al., 2005; Sotiriou et al., 2006). As summarized in Figure 7A, expression levels of the 18 proinvasion genes were able to stratify patients by K-means clustering into two subgroups with significant differences in metastasis-free or recurrence-free survival by Kaplan-Meier survival analysis in all 3 independent data sets. Moreover, by C statistics these 18 genes were comparable to the 70 genes in the FDA-approved MammaPrint® in their ability to prognosticate recurrence or metastasis (Figure 7B). These data are remarkable in light of the fact that these genes were discovered in melanoma. Such cross-tumor prognostic significance reinforces the human relevance and highlights the power of this integrative functional genomics approach for discovery of metastasis oncogenes that can function across different tumor types.

DISCUSSION

In this study we employed well-defined GEM models, comparative oncogenomics, and functional genomics to identify genes capable of driving invasion and transformation in early-staged melanomas. The genomic and biological homogeneity of GEM tumors and filtering power of cross-species comparisons proved highly effective in generating a shorter, more biologically significant list of genes enriched for cancer- and metastasis-relevant networks than either human or mouse data sets alone. Subsequent functional screen and stringent validation efforts identified high-priority drivers of invasion—the key biological process that correlates with metastatic potential in melanoma. Finally,

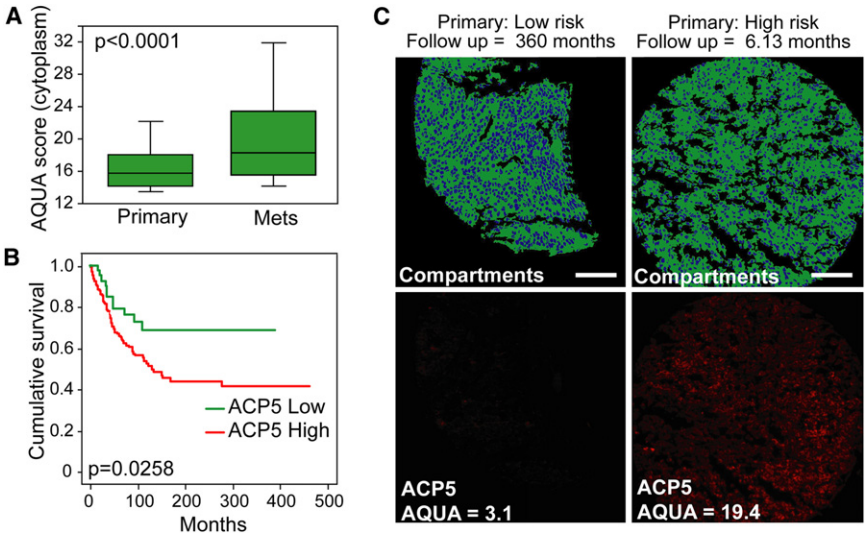

Figure 5. Acp5 Expression on Melanoma Tissue Microarrays

(A) Box plot demonstrating the distribution of Acp5 cytoplasmic scores for primary (n = 182) and metastatic (n = 325) lesions on the Yale Melanoma Outcome Annotated TMA (YTMA59). p value calculated by mixed-model ANOVA. Error bars indicate data within 1.5 interquartile range of the mean.

(B) Primary tumors from (A) were divided into quartiles based on cytoplasmic expression of Acp5. Comparison of melanoma-specific survival of the lowest quartile (green) with the other three quartiles (red) is shown. p value calculated by log rank test.

(C) Representative staining of Acp5 (red) across histospot tumor specimens on YTMA59. S100/GP100 (green) defines tumor and nonnuclear compartments, and DAPI (blue) defines the nuclear compartments. Scale bars, 100 μm.

See also Figure S5.

although oncogenic activity was not screened for, it is remarkable that every one of the six proinvasion genes is robustly transforming in vivo, a finding that supports the hypothesis that drivers of metastasis in early-staged primary tumors also serve as professional oncogenes promoting tumorigenesis.

Of the six validated metastasis oncogenes, most are not known or implicated in metastasis, although some have been linked to cancer. For example, *HSF1* (Heat Shock Factor 1) is a regulator of cell transformation and in vivo tumorigenesis (Dai et al., 2007), and *HSF1*-deficient cells exhibit markedly impaired migration and MAP kinase signaling (O'Callaghan-Sunol and Sherman, 2006). In a transgenic mouse model with overexpression of *NDC80*, a component of the spindle checkpoint, tumor development was reported in multiple organs (Diaz-Rodriguez et al., 2008), and depletion of *NDC80* impairs tumor growth (Gurzov and Izquierdo, 2006). *HOXA1* (Homeobox Transcription factor 1) has oncogenic activity in mammary tumor models (Zhang et al., 2003) and is upregulated in multiple human cancers, including breast, squamous cell carcinoma, and melanoma (Chariot and Castronovo, 1996; Maeda et al., 2005; Abe et al., 2006). *VSIG4* (V-set and immunoglobulin domain containing 4) is a cell surface protein whose expression is mainly restricted to macrophages where it functions as a potent T cell inhibitor (Vogt et al., 2006; Xu et al., 2010). Based on its significantly higher expression in aggressive breast and ovarian tissues compared to benign tissues, *ACP5* expression has been suggested to represent a progression marker (Honig et al., 2006; Adams et al., 2007), consistent with our data in melanoma. Although we have shown in model systems that *ACP5* overexpression alone was sufficient in conferring distal metastasis in vivo, frank metastasis in patients most certainly requires cooperation of a multitude of genetic alterations, each driving one or more steps in the metastatic cascade. Therefore, one may speculate that there would be metastasis oncogenes that are drivers of other biological processes (besides invasion) that are required for metastasis; thus, a similar integrated functional genomics approach could be powerful in aiding their discovery.

The majority of cancer-related deaths result from metastases. With the improvement of early detection capability by serum biomarkers and imaging advances, an increasing number of cancer cases will be diagnosed and surgically resected prior to apparent metastatic spread, leading to better overall survival relative to high-stage disease. At the same time, it is long recognized that equivalent low-stage cancers are clinically heterogeneous with a subset exhibiting high-risk behavior, recurring with metastatic spread in the years ahead. The precise identification of such high-risk cases would enable more aggressive management in adjuvant setting, while avoiding unnecessary treatment in those patients cured by surgical intervention alone. Therefore, there is a growing need for the development of molecular-based prognostic biomarkers that can stratify risk for metastasis in the early-stage cancer population that constitutes an increasing proportion of cancer diagnoses each year. Transcriptomic and genomic characterization of human cancers supports the presence of molecular signals resident in primary tumors that can predict risk for metastasis. The development of MammaPrint® and OncotypeDx® has provided a strong measure of clinical proof of this concept. In comparison to the predominantly statistical correlative analyses from which these signatures were derived, the approach reported here focuses on discovery of functional drivers of the metastatic process that are also oncogenic in early-stage cancers. Given their functional nature, we believe that the mechanism-of-action through which these proinvasion oncogenes drive metastasis would inform evidence-based therapeutic decisions in the adjuvant setting, in addition to themselves being rational points for therapeutic intervention. In this regard the convergence of emerging targeted therapeutics for melanoma (such as the selective BRAF inhibitor) and identification of proinvasion oncogenes as prognostic biomarkers (such as *ACP5*) will offer a real opportunity to stratify a molecularly high-risked subpopulation among patients with early-stage primary melanoma for clinical investigation aimed to explore the efficacy of these new therapies in the prevention of recurrence and metastasis.

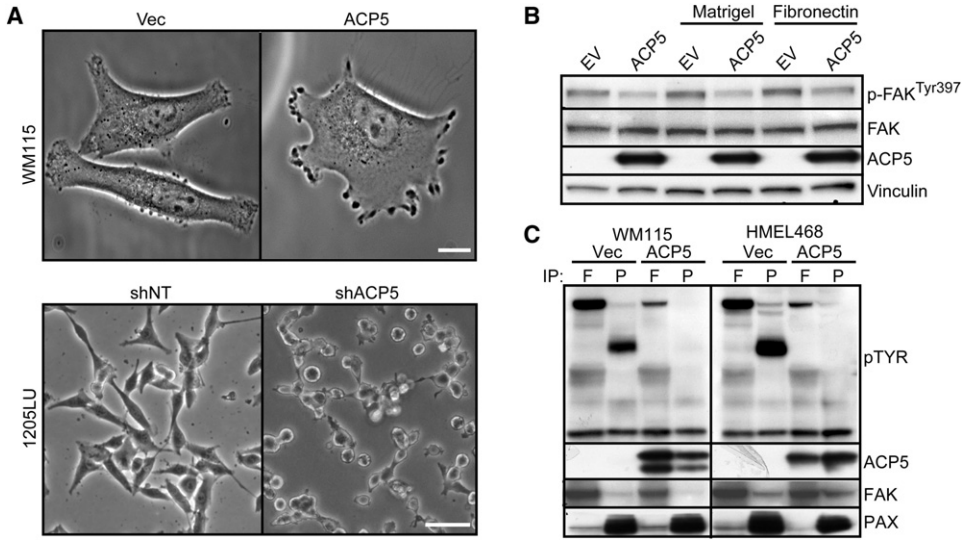

Figure 6. *ACP5* Expression Modulates Phosphorylation Status of Adhesion Molecules

(A) Morphology of WM115 (top) cells without (Vec) or with *ACP5* overexpression, or 1205Lu cells (bottom) treated with a control shRNA (shNT) or an shRNA targeting *ACP5* (shACP5). Scale bars, 10 μm (top) and 5 μm (bottom).

(B) Immunoblot analysis of indicated proteins of WM115 cells expressing empty vector (EV) or *ACP5* and grown on plates without coating or coated with Matrigel or fibronectin as indicated.

(C) Protein lysates extracted from WM115 and HMEL468 cells were immunoprecipitated (IP) with antibodies against FAK (or F) and PAX (or P) for immunoblotting with the indicating antibodies. Tyrosine phosphorylation (pTyr) is determined by anti-pTyr immunoblot analysis.

See also Figure S6, and Movies S1 and S2.

EXPERIMENTAL PROCEDURES

GEM Models for Melanoma, Comparative Data Analyses, and In Vivo Tumor Assays

All mice were bred and maintained under defined conditions at the Dana-Farber Cancer Institute (DFCI), and all procedures were approved by the Animal Care and Use Committee of DFCI and conformed to the legal mandates and national guidelines for the care and maintenance of laboratory animals. The tetracycline-inducible *MET*-driven mouse model (iMet) was constructed similarly to the previously described iHRAS* model (Chin et al., 1999). Mice were sacrificed according to institute guidelines, and organs were fixed in 10% buffered formalin and paraffin embedded. Tissue sections were stained with H&E to enable classification of the lesions and detection of tumor metastasis. For detection of Met protein, tumor sections were immunostained with total Met and phospho Met (Tyr1349) antibodies (Cell Signaling Technology). iMet tumors were additionally immunostained with S100 antibody (Sigma). RNA from cutaneous melanomas derived from iMet or iHRAS* models was profiled on Affymetrix Gene Chips, and resultant transcriptomes were compared using Significance Analysis of Microarray (SAM 2.0) to generate a phenotype-based (metastatic capable or not) differentially expressed gene list. Cross-species triangulation to human gene expression and CNAs was based on ortholog mapping. See Supplemental Experimental Procedures for more details.

For xenograft tumorigenicity studies, HMEL468 cells were transduced with pLenti6/V5 DEST-generated virus for stable expression of GFP (control) or the indicated genes. Following selection with blasticidin (Invitrogen; 5 μg/ml) for 5–7 days, 1.0 × 10^6 cells (prepared in Hank's balanced salts [HBSs] at 1:1 with Matrigel) were injected subcutaneously into the right flank of NCr-Nude (Taconic) mice. Two-tailed Student's t test calculations were performed using Prism 4 (GraphPad). In vivo metastasis assays were performed by: (1) subcutaneous skin tumor assays using 1205Lu cells stably expressing GFP (control) or *ACP5*; and (2) orthotopic mammary fat pad assays using nonmetastatic NB008 adenocarcinoma cells stably expressing vector (control) or *ACP5*, as described in Supplemental Experimental Procedures.

Cell Culture

HMEL468 primed melanocytes were a subclone of PMEL/hTERT/CDK4(R24C)/p53DD/$BRAF^{V600E}$ cells, as described (Garraway et al., 2005). The nonmetastatic NB008 cell line was established from a spontaneous tumor isolated from the breast of a G4 52-week-old female $mTerc^{-/-}$, $p53^{+/-}$ mouse. GFP-mTerc was reintroduced into the resulting cell line by lentiviral transduction prior to use in these studies. The WM115 melanoma cell line was obtained from the Wistar Institute, and the 1205Lu melanoma cell line was obtained from the American Type Culture Collection. M619 and C918 melanoma lines have been described previously (Maniotis et al., 1999). All cell lines were propagated at 37°C and 5% CO_2 in humidified atmosphere in RPMI 1640 medium supplemented with 10% FBS.

Invasion Screen and Transwell Invasion Assays

The low-complexity genetic screen for cell invasion was performed using Tert-immortalized melanocytes HMEL468 in 96-well modified Boyden chambers coated with Matrigel (96-well tumor invasion plates; BD Bioscience) following the manufacturer's recommendations. Invaded cells were detected with labeling using 4 μM Calcein AM (BD Bioscience) and measured by fluorescence at 494/517 nm (Abs/Em) after 20 hr incubation at 37°C and 5% CO_2. Positive-scoring candidates were identified as those scoring 2× standard deviations from the vector control. See Supplemental Experimental Procedures for details on the screen and individual clones. Validation assays for cell invasion were performed in standard 24-well invasion chambers containing Matrigel following the manufacturer's recommendations. Following 20 hr incubation at 37°C and 5% CO_2, chambers were fixed in 10% formalin and stained with crystal violet for manual counting or by pixel quantitation with Adobe Photoshop (Adobe). Data were normalized to input cells to control for differences in cell number (loading control).

AQUA

Use of human tissues in this study is approved by the Yale institutional IRB, HIC protocol number 9500008219 including consent and waived consent. AQUA, Yale Melanoma Arrays, and tissue microarray construction have been described previously (Camp et al., 2002; Gould Rothberg et al., 2009).

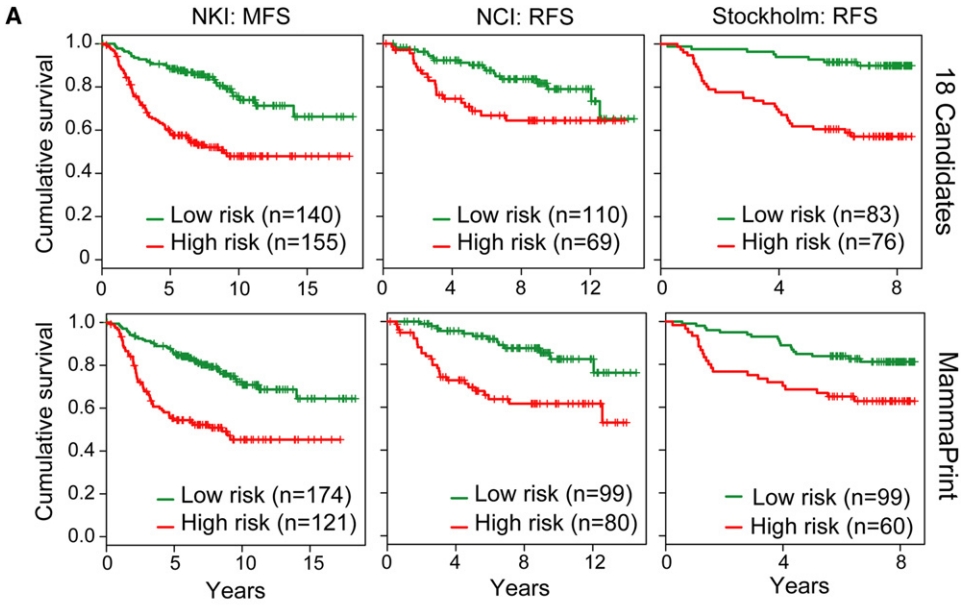

B

	NKI: MFS			NCI: RFS			Stockholm: RFS		
Signature	P	HR	C	P	HR	C	P	HR	C
18 Candidates	1.70E-07	3.00	0.790	1.90E-02	2.07	0.725	1.40E-06	5.49	0.853
MammaPrint 70 genes	2.30E-07	2.74	0.767	1.80E-04	3.30	0.819	4.60E-03	2.39	0.721

Figure 7. Kaplan-Meier Survival Curves in Breast Cancer Cohorts

(A) K-means clustering analysis based on the 18 gene proinvasion oncogene (top) and MammaPrint (bottom) signature using three independent cohorts of early-staged breast cancers: NKI metastasis-free survival (MFS) (van de Vijver et al., 2002); NCI recurrence-free survival (RFS) (Sotiriou et al., 2006); and Stockholm RFS (Pawitan et al., 2005). p values calculated by log rank test.

(B) Comparison of the 18-gene signature performance with the MammaPrint (Agendia, Huntington Beach, CA, USA) prognostic signature using the patient cohorts specified in (A). HR, hazard ratio; C, C statistics.

Arrays were stained with the following antibodies: monoclonal anti-Fscn1 diluted 1:500 (clone 55K2; Santa Cruz Biotechnology, Inc.); polyclonal anti-Hoxa1 diluted 1:50 (BO1P; Abnova); polyclonal anti-Hsf1 diluted 1:2500 (AO1; Abnova); monoclonal anti-Ndc80 diluted 1:50 (clone 1A10; Abnova); monoclonal anti-Acp5 diluted 1:100 (clone 26E5; Abcam); polyclonal anti-Ncaph diluted 1:750 (Bethyl Laboratories, Inc.); and polyclonal anti-Vsig4 diluted 1:1000 (ab56037; Abcam). See Supplemental Experimental Procedures for full details.

Anchorage-Independent Growth Assays

Soft-agar colony formation assays were performed on 6-well plates in triplicate for cells transduced with pLKO-shGFP (Open Biosystems) or shRNA (Bill Hahn, DFCI/Broad Institute; available via Open Biosystems) hairpins targeting the indicated genes (see Supplemental Experimental Procedures for additional clone information). Cells were selected for 5 days with 2.5 μg/μl puromycin, and 1 × 10^4 cells were mixed thoroughly in cell growth medium containing 0.4% SeaKem LE agarose (Fisher) in RPMI plus 10% FBS, followed by plating onto bottom agarose prepared with 0.65% agarose in RPMI plus 10% FBS. Each well was allowed to solidify and subsequently covered in 1 ml RPMI plus 10% FBS plus P/S, which was refreshed every 4 days. Colonies were stained with 0.05% (wt/vol) iodonitrotetrazolium chloride (Sigma) and scanned at 1200 dpi using a flatbed scanner, followed by counting and two-tailed Student's t test calculation using Prism 4 (GraphPad). Verification of knockdown was achieved by qRT-PCR (described in Supplemental Experimental Procedures) using gene-specific primer sets (SABiosciences).

Coimmunoprecipitation and Immunoblotting

For immunoprecipitation studies, lysates were prepared in NP-40 buffer (20 mM Tris-HCl [pH 8.0], 150 mM NaCl, 2 mM EDTA, 1% NP-40) containing 1 mM PMSF, 1× Protease Inhibitor Cocktail (Roche), and 1× Phosphatase inhibitor (Calbiochem) for immunoprecipitation. Anti-Paxillin (Abcam) or anti-FAK (Santa Cruz Biotechnology) antibody was added to cell lysates for 2 hr at 4°C with rocking, followed by incubation overnight with protein G sepharose (Roche) at 4°C with rocking. Immunoprecipitates were washed three times for 10 min with lysis buffer, eluted by the addition of SDS loading buffer after centrifugation, and resolved on NuPAGE 4%–12% Bis-Tris gels (Invitrogen) for immunoblotting on PVDF (Millipore). The following antibodies were used for immunoblotting following the manufacturer's recommendations: anti-FAK (Santa Cruz Biotechnology); anti-FAK (Tyr397; Cell Signaling); anti-Paxillin (Abcam); anti-Paxillin (Tyr118; Cell Signaling); anti-Vinculin (Santa Cruz Biotechnology); anti-V5 (for Acp5 detection; Invitrogen); and anti-phosphotyrosine (Millipore).

Cell Imaging

Single-plane phase image was collected on a Nikon Ti with a 40× Plan-Apochromatic phase objective NA 0.95 and a Clara camera using Andor iQ software (Andor Technology). Time-lapse phase images were collected on a Nikon TE2000-E with a 10× phase objective and an OrcaER camera (Hamamatsu) at the DFCI Confocal and Light Microscopy Core. Shutters, stage position, and camera were controlled by NIS-Elements software (Nikon, Melville, NY). Images were collected every 2 min at 6–12 stage positions for 20 hr. A representative time-lapse movie for vector and *ACP5*-overexpressing cells

are shown. For the QuickTime® movie, every tenth frame was used (20 min time points) and playback is 15 frames per second.

Breast Cancer Prognostic Studies

Expression patterns of the 18 candidate preinvasion oncogenes and MammaPrint® 70-gene signature (Agendia, Huntington Beach, CA, USA) were used for Kaplan-Meier survival analyses of the indicated breast cancer data sets by K-means clustering using the survival package in R.

ACCESSION NUMBERS

Expression array data for the iMet and iHRAS* tumors generated by these studies have been deposited into the GEO database with accession number GSE29074.

SUPPLEMENTAL INFORMATION

Supplemental Information includes Supplemental Experimental Procedures, six figures, four tables, and two movies and can be found with this article online at doi:10.1016/j.ccr.2011.05.025.

ACKNOWLEDGMENTS

Genomic studies and analyses were performed by the Belfer Institute for Applied Cancer Science. The authors wish to thank members of the Chin laboratory for helpful discussion, particularly Shan Jiang for mouse colony work and Bob Xiong for computational assistance. The authors acknowledge the generous gifts of ORF clones provided by Drs. Marc Vidal and David Hill of the human ORFeome in Center for Cancer System Biology, and the HMEL468 primed melanocytes (PMEL/hTERT/CDK4(R24C)/p53DD/BRAF^{V600E}) provided by Dr. David Fisher. Wide-field microscopy images for this study were acquired in the Confocal and Light Microscopy Core Facility at the Dana-Farber Cancer Institute. K.L.S. was supported by a postdoctoral fellowship from the American Cancer Society and was previously supported by a National Institutes of Health Training Grant appointment in the Department of Dermatology at Brigham and Women's Hospital, Boston. C.N. was supported by a fellowship from FCT (Praxis XXI/BD/21794/99). R.v.D. was supported by a KWF fellowship for medical specialists. This work is supported by grants from the NIH (RO1 CA93947, U01 CA84313, and P50 CA93683), and by an Established Investigator Award from the Melanoma Research Foundation to L.C. L.C. is the recipient of the Abby S. & Howard P. Milstein Innovation Award by American Skin Association. Technology/intellectual property pertaining to this manuscript has been exclusively licensed to Metamark Genetics, a development-stage molecular diagnostics company cofounded by L.C., D.L.R., and R.A.D. D.L.R. is cofounder, stockholder in, and consultant to HistoRx, the exclusive licensee of the Yale held patent on the AQUA technology that was used in this work.

Received: November 12, 2010
Revised: April 28, 2011
Accepted: May 28, 2011
Published: July 11, 2011

REFERENCES

Abe, M., Hamada, J., Takahashi, O., Takahashi, Y., Tada, M., Miyamoto, M., Morikawa, T., Kondo, S., and Moriuchi, T. (2006). Disordered expression of HOX genes in human non-small cell lung cancer. Oncol. Rep. *15*, 797–802.

Adams, L.M., Warburton, M.J., and Hayman, A.R. (2007). Human breast cancer cell lines and tissues express tartrate-resistant acid phosphatase (TRAP). Cell Biol. Int. *31*, 191–195.

Berger, A.J., Davis, D.W., Tellez, C., Prieto, V.G., Gershenwald, J.E., Johnson, M.M., Rimm, D.L., and Bar-Eli, M. (2005). Automated quantitative analysis of activator protein-2alpha subcellular expression in melanoma tissue microarrays correlates with survival prediction. Cancer Res. *65*, 11185–11192.

Bernards, R., and Weinberg, R.A. (2002). A progression puzzle. Nature *418*, 823.

Camp, R.L., Chung, G.G., and Rimm, D.L. (2002). Automated subcellular localization and quantification of protein expression in tissue microarrays. Nat. Med. *8*, 1323–1327.

Capeller, B., Caffier, H., Sutterlin, M.W., and Dietl, J. (2003). Evaluation of tartrate-resistant acid phosphatase (TRAP) 5b as serum marker of bone metastases in human breast cancer. Anticancer Res. *23*, 1011–1015.

Chariot, A., and Castronovo, V. (1996). Detection of HOXA1 expression in human breast cancer. Biochem. Biophys. Res. Commun. *222*, 292–297.

Chen, L., Yang, S., Jakoncic, J., Zhang, J.J., and Huang, X.Y. (2010). Migrastatin analogues target fascin to block tumour metastasis. Nature *464*, 1062–1066.

Chin, K., de Solorzano, C.O., Knowles, D., Jones, A., Chou, W., Rodriguez, E.G., Kuo, W.L., Ljung, B.M., Chew, K., Myambo, K., et al. (2004). In situ analyses of genome instability in breast cancer. Nat. Genet. *36*, 984–988.

Chin, L., Pomerantz, J., Polsky, D., Jacobson, M., Cohen, C., Cordon-Cardo, C., Horner, J.W., 2nd, and DePinho, R.A. (1997). Cooperative effects of INK4a and ras in melanoma susceptibility in vivo. Genes Dev. *11*, 2822–2834.

Chin, L., Tam, A., Pomerantz, J., Wong, M., Holash, J., Bardeesy, N., Shen, Q., O'Hagan, R., Pantginis, J., Zhou, H., et al. (1999). Essential role for oncogenic Ras in tumour maintenance. Nature *400*, 468–472.

Dai, C., Whitesell, L., Rogers, A.B., and Lindquist, S. (2007). Heat shock factor 1 is a powerful multifaceted modifier of carcinogenesis. Cell *130*, 1005–1018.

Diaz-Rodriguez, E., Sotillo, R., Schvartzman, J.M., and Benezra, R. (2008). Hec1 overexpression hyperactivates the mitotic checkpoint and induces tumor formation in vivo. Proc. Natl. Acad. Sci. USA *105*, 16719–16724.

Ganss, R., Montoliu, L., Monaghan, A.P., and Schutz, G. (1994). A cell-specific enhancer far upstream of the mouse tyrosinase gene confers high level and copy number-related expression in transgenic mice. EMBO J. *13*, 3083–3093.

Garraway, L.A., Widlund, H.R., Rubin, M.A., Getz, G., Berger, A.J., Ramaswamy, S., Beroukhim, R., Milner, D.A., Granter, S.R., Du, J., et al. (2005). Integrative genomic analyses identify MITF as a lineage survival oncogene amplified in malignant melanoma. Nature *436*, 117–122.

Gossen, M., Freundlieb, S., Bender, G., Muller, G., Hillen, W., and Bujard, H. (1995). Transcriptional activation by tetracyclines in mammalian cells. Science *268*, 1766–1769.

Gould Rothberg, B.E., Berger, A.J., Molinaro, A.M., Subtil, A., Krauthammer, M.O., Camp, R.L., Bradley, W.R., Ariyan, S., Kluger, H.M., and Rimm, D.L. (2009). Melanoma prognostic model using tissue microarrays and genetic algorithms. J. Clin. Oncol. *27*, 5772–5780.

Gupta, G.P., and Massague, J. (2006). Cancer metastasis: building a framework. Cell *127*, 679–695.

Gurzov, E.N., and Izquierdo, M. (2006). RNA interference against Hec1 inhibits tumor growth in vivo. Gene Ther. *13*, 1–7.

Halleen, J.M., Alatalo, S.L., Janckila, A.J., Woitge, H.W., Seibel, M.J., and Vaananen, H.K. (2001). Serum tartrate-resistant acid phosphatase 5b is a specific and sensitive marker of bone resorption. Clin. Chem. *47*, 597–600.

Hanahan, D., and Weinberg, R.A. (2011). Hallmarks of cancer: the next generation. Cell *144*, 646–674.

Hashimoto, Y., Skacel, M., and Adams, J.C. (2005). Roles of fascin in human carcinoma motility and signaling: prospects for a novel biomarker? Int. J. Biochem. Cell Biol. *37*, 1787–1804.

Honig, A., Rieger, L., Kapp, M., Krockenberger, M., Eck, M., Dietl, J., and Kammerer, U. (2006). Increased tartrate-resistant acid phosphatase (TRAP) expression in malignant breast, ovarian and melanoma tissue: an investigational study. BMC Cancer *6*, 199.

Hussussian, C.J., Struewing, J.P., Goldstein, A.M., Higgins, P.A., Ally, D.S., Sheahan, M.D., Clark, W.H., Jr., Tucker, M.A., and Dracopoli, N.C. (1994). Germline p16 mutations in familial melanoma. Nat. Genet. *8*, 15–21.

Izumchenko, E., Singh, M.K., Plotnikova, O.V., Tikhmyanova, N., Little, J.L., Serebriiskii, I.G., Seo, S., Kurokawa, M., Egleston, B.L., Klein-Szanto, A., et al. (2009). NEDD9 promotes oncogenic signaling in mammary tumor development. Cancer Res. *69*, 7198–7206.

Kabbarah, O., Nogueira, C., Feng, B., Nazarian, R.M., Bosenberg, M., Wu, M., Scott, K.L., Kwong, L.N., Xiao, Y., Cordon-Cardo, C., et al. (2010). Integrative genome comparison of primary and metastatic melanomas. PLoS One *5*, e10770.

Kamb, A., Gruis, N.A., Weaver-Feldhaus, J., Liu, Q., Harshman, K., Tavtigian, S.V., Stockert, E., Day, R.S., 3rd, Johnson, B.E., and Skolnick, M.H. (1994). A cell cycle regulator potentially involved in genesis of many tumor types. Science *264*, 436–440.

Kim, M., Gans, J.D., Nogueira, C., Wang, A., Paik, J.H., Feng, B., Brennan, C., Hahn, W.C., Cordon-Cardo, C., Wagner, S.N., et al. (2006). Comparative oncogenomics identifies NEDD9 as a melanoma metastasis gene. Cell *125*, 1269–1281.

Lyubimova, N.V., Pashkov, M.V., Tyulyandin, S.A., Gol'dberg, V.E., and Kushlinskii, N.E. (2004). Tartrate-resistant acid phosphatase as a marker of bone metastases in patients with breast cancer and prostate cancer. Bull. Exp. Biol. Med. *138*, 77–79.

Maeda, K., Hamada, J., Takahashi, Y., Tada, M., Yamamoto, Y., Sugihara, T., and Moriuchi, T. (2005). Altered expressions of HOX genes in human cutaneous malignant melanoma. Int. J. Cancer *114*, 436–441.

Maniotis, A.J., Folberg, R., Hess, A., Seftor, E.A., Gardner, L.M., Pe'er, J., Trent, J.M., Meltzer, P.S., and Hendrix, M.J. (1999). Vascular channel formation by human melanoma cells in vivo and in vitro: vasculogenic mimicry. Am. J. Pathol. *155*, 739–752.

O'Callaghan-Sunol, C., and Sherman, M.Y. (2006). Heat shock transcription factor (HSF1) plays a critical role in cell migration via maintaining MAP kinase signaling. Cell Cycle *5*, 1431–1437.

O'Neill, G.M., Seo, S., Serebriiskii, I.G., Lessin, S.R., and Golemis, E.A. (2007). A new central scaffold for metastasis: parsing HEF1/Cas-L/NEDD9. Cancer Res. *67*, 8975–8979.

Paik, S., Shak, S., Tang, G., Kim, C., Baker, J., Cronin, M., Baehner, F.L., Walker, M.G., Watson, D., Park, T., et al. (2004). A multigene assay to predict recurrence of tamoxifen-treated, node-negative breast cancer. N. Engl. J. Med. *351*, 2817–2826.

Pawitan, Y., Bjohle, J., Amler, L., Borg, A.L., Egyhazi, S., Hall, P., Han, X., Holmberg, L., Huang, F., Klaar, S., et al. (2005). Gene expression profiling spares early breast cancer patients from adjuvant therapy: derived and validated in two population-based cohorts. Breast Cancer Res. *7*, R953–R964.

Perou, C.M., Sorlie, T., Eisen, M.B., van de Rijn, M., Jeffrey, S.S., Rees, C.A., Pollack, J.R., Ross, D.T., Johnsen, H., Akslen, L.A., et al. (2000). Molecular portraits of human breast tumours. Nature *406*, 747–752.

Ramaswamy, S., Ross, K.N., Lander, E.S., and Golub, T.R. (2003). A molecular signature of metastasis in primary solid tumors. Nat. Genet. *33*, 49–54.

Rudolph, K.L., Millard, M., Bosenberg, M.W., and DePinho, R.A. (2001). Telomere dysfunction and evolution of intestinal carcinoma in mice and humans. Nat. Genet. *28*, 155–159.

Sanz-Moreno, V., Gadea, G., Ahn, J., Paterson, H., Marra, P., Pinner, S., Sahai, E., and Marshall, C.J. (2008). Rac activation and inactivation control plasticity of tumor cell movement. Cell *135*, 510–523.

Sotiriou, C., Wirapati, P., Loi, S., Harris, A., Fox, S., Smeds, J., Nordgren, H., Farmer, P., Praz, V., Haibe-Kains, B., et al. (2006). Gene expression profiling in breast cancer: understanding the molecular basis of histologic grade to improve prognosis. J. Natl. Cancer Inst. *98*, 262–272.

van de Vijver, M.J., He, Y.D., van't Veer, L.J., Dai, H., Hart, A.A., Voskuil, D.W., Schreiber, G.J., Peterse, J.L., Roberts, C., Marton, M.J., et al. (2002). A gene-expression signature as a predictor of survival in breast cancer. N. Engl. J. Med. *347*, 1999–2009.

van't Veer, L.J., Dai, H., van de Vijver, M.J., He, Y.D., Hart, A.A., Mao, M., Peterse, H.L., van der Kooy, K., Marton, M.J., Witteveen, A.T., et al. (2002). Gene expression profiling predicts clinical outcome of breast cancer. Nature *415*, 530–536.

Vogt, L., Schmitz, N., Kurrer, M.O., Bauer, M., Hinton, H.I., Behnke, S., Gatto, D., Sebbel, P., Beerli, R.R., Sonderegger, I., et al. (2006). VSIG4, a B7 family-related protein, is a negative regulator of T cell activation. J. Clin. Invest. *116*, 2817–2826.

Xu, S., Sun, Z., Li, L., Liu, J., He, J., Song, D., Shan, G., Liu, H., and Wu, X. (2010). Induction of T cells suppression by dendritic cells transfected with VSIG4 recombinant adenovirus. Immunol. Lett. *128*, 46–50.

Zhang, X., Zhu, T., Chen, Y., Mertani, H.C., Lee, K.O., and Lobie, P.E. (2003). Human growth hormone-regulated HOXA1 is a human mammary epithelial oncogene. J. Biol. Chem. *278*, 7580–7590.

Zheng, Y., and Lu, Z. (2009). Paradoxical roles of FAK in tumor cell migration and metastasis. Cell Cycle *8*, 3474–3479.